Chinese Chemical Letters 34 (2023) 107541

Contents lists available at ScienceDirect

Chinese Chemical Letters

journal homepage: www.elsevier.com/locate/cclet

Pyrylium-based porous organic polymers *via* Knoevenagel condensation for efficient visible-light-driven heterogeneous photodegradation

Renwei Hu[a], Mehdi Hassan[c,*], Lu Liu[a], Shuguang Zhang[a], Weitao Gong[a,b,*]

[a] State Key Laboratory of Fine Chemicals, School of Chemical Engineering, Dalian University of Technology, Dalian 116024, China
[b] Engineering Laboratory of Boric and Magnesic Functional Material Preparative and Applied Technology, Dalian 116024, China
[c] Department of Chemistry, University of Baltistan, Skardu 16100, Pakistan

ARTICLE INFO

Article history:
Received 11 April 2022
Revised 8 May 2022
Accepted 17 May 2022
Available online 21 May 2022

Keywords:
Ionic porous organic polymer
Pyryliun salts
Knoevenagel reaction
Vinylene-linked
Photodegradation

ABSTRACT

Pyrylium salts are a type of representative and convincing example of versatility and variety not only as a nodal point in organic transformations but also as an attractive building block in functional organic materials. Herein, we report an effective synthetic protocol to fabricate a new pyrylium-containing porous organic polymers (POPs), named TMP-P, *via* Knoevenagel condensation with 2,4,6-trimethylpyrylium salt (TMP) as the key building block and 1,4-phthalaldehyde as the linker. The resulting ionic polymer TMP-P exhibited efficient visible-light-driven heterogeneous photodegradation of Rhodamine B, owing to the presence of wide visible light absorption and a narrow optical band gap triggered pyrylium core in the framework.

Pyrylium salts are ionic organic dyes firstly reported by Baeyer in 1911, which consist of six-membered heterocycles with a positively charged oxygen atom [1]. This unique molecular structure makes pyrylium salts a representative and convincing example of versatility and variety not only as a nodal point in organic transformations but also as an attractive building block in functional organic materials. Pyrylium salts have broad absorption in UV-vis and visible region, appropriate excited state redox potential, higher intersystem crossing quantum yield, and longer triplet lifetime. There is no net charge separation in its single electron transfer process, which enhanced the formation of free-radical ions and took place in charge exchanges, whereas back electron transfer (BET) is reduced [2]. Owing to above mentioned unique photophysical properties among other organic dyes, pyrylium salts have been widely utilized as efficient metal-free photocatalysts in the degradation of pollutants [3–6], organic conversions [7–11], even cationic [12–14], free-radical photopolymerization [15] and ring-opening metathesis polymerization (ROMP) [16]. However, the poor chemical stability and low reusability of pyrylium salts restrict its further wide applications. In this regard, the immobilization of pyrylium salts into a certain network to form heterogeneous catalysts might be a feasible strategy to overcome the challenges.

Porous organic polymers (POPs) have recently emerged as an effective platform to construct heterogeneous photocatalysts owing to the advantages of high specific surface area, low skeleton density, high porosity, and constant physical and chemical behaviors [17–19]. Incorporating photocatalytic moiety into POPs has been proved to be a promising strategy to design and construct heterogeneous photocatalysts. Therefore, various new POPs associated with active organic building blocks, *e.g.*, phthalocyanine [20], isoindigo blue [21], BODIPY [22], Boranil [23], β-diketone boron difluoride [24] and carbazole [25], as have been developed with substantial photocatalytic performance in CO_2 reduction [26], degradation of organic dyes [27] and organic transformations [28]. Conversely, less consideration has been paid to introducing pyrylium salts as a key moiety with POPs [29] to construct corresponding photodegradation catalysts.

Therefore, due to continuous research findings in the field of pyrylium chemistry [30–32], here, we designed and prepared a new pyrylium-based POPs by using 2,4,6-trimethylpyrylium salt used as a key building block while 1,4-phthalaldehyde used as a linker *via* Knoevenagel condensation with no catalyst. The resulting TMP-P exhibited wider visible light absorption and a narrower optical bandgap compared with the relevant model compound TMP-M. Furthermore, TMP-P was successfully employed as a

* Corresponding authors.
E-mail addresses: mehdi.hassan@uobs.edu.pk (M. Hassan), wtgong@dlut.edu.cn (W. Gong).

https://doi.org/10.1016/j.cclet.2022.05.055
1001-8417/

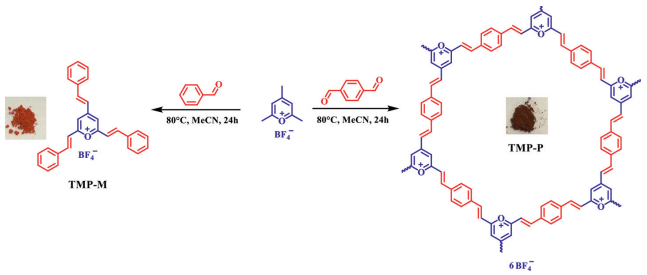

Scheme 1. The synthesis of TMP-M and TMP-P.

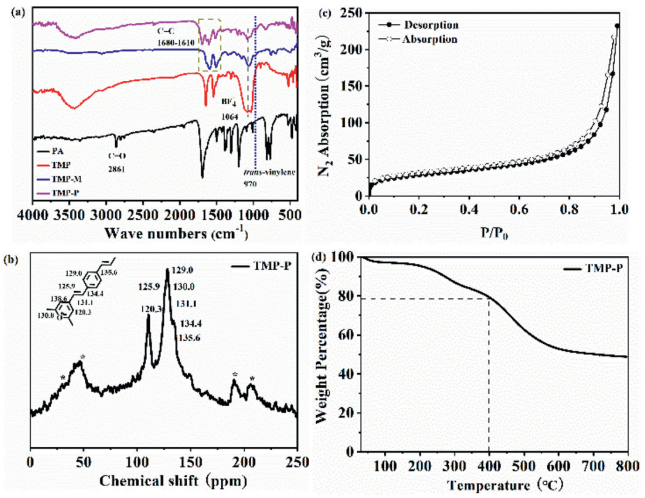

Fig. 1. (a) FT-IR spectra of PA (black), TMP (red), TMP-M (blue), TMP-P (pink). (b) ^{13}C CP-MAS NMR spectra of TMP-P, *denote spinning sidebands. (c) N_2 sorption isotherms of TMP-P at 77 K. (d) Thermogravimetric analysis of TMP-P.

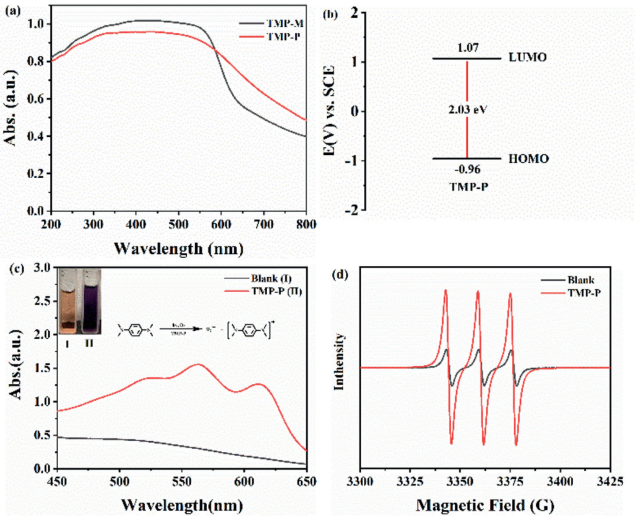

Fig. 2. (a) UV-vis diffuse reflectance spectra of TMP-P (red) and TMP-M (black). (b) Schematic energy band structure of TMP-P. (c) UV-vis absorption spectra and photographs of TMPD in H_2O in the presence (black) and the absence (red) of TMP-P upon irradiation by visible light (10 W blue LED). (d) The EPR spectra of TMP-P in the presence of air and TEMP.

heterogeneous photocatalyst in the photodegradation of Rhodamine B (RhB) with superior photocatalytic performance as compared to TMP and TMP-M. These results revealed that the pyrylium salts as proficient moiety for constructing new POPs-based metal-free photocatalysts and validated the pyrylium chemistry as a promising synthetic strategy to fabricate new POPs with versatile functions.

The synthetic routes towards TMP-M and TMP-P were shown in Scheme 1. Firstly, the Knoevenagel condensation reaction of 2,4,6-trimethylpyrylium tetrafluoroborate (TMP) with benzaldehyde was taken as a pilot reaction to synthesize 2,4,6-tristyrylpyrylium tetrafluoroborate (TMP-M) as the model compound. Likewise, polymer TMP-P was also synthesized by a similar procedure: 2,4,6-trimethylpyrylium tetrafluoroborate (TMP, 1 mmol, 210 mg), 1,4-phthalaldehyde (PA, 1.5 mmol, 200 mg) and acetonitrile (3 mL) were added directly into the polytetrafluoroethylene (PTFE) liner. The PTFE liner was put into the hydrothermal reactor and reacted in an oven at 80 °C for 24 h. After cooling down the reaction mixture, the precipitation was filtered and washed with dichloromethane, acetone, *N*,*N*-dimethylformamide, tetrahydrofuran, and methanol several times. Further purification was taken by Soxhlet extractor with THF solvent for 24 h and dried in a vacuum at 70 °C for 12 h to get the red polymer TMP-P (290 mg, 70%).

The structure of TMP-P was initially analyzed by FT-IR (Fig. 1a). The C=O absorption band exhibited at 2861 cm^{-1} in PA, was not observed in products shown in Fig. 1a. Besides, TMP-M and TMP-P showed C=C absorption bands at 1610-1680 cm^{-1}, and 970 cm^{-1}, and these results strongly indicated the formation of vinylene linkage. The BF_4^- bands in products at 1064 cm^{-1} proved the retention of the pyrylium ring. Furthermore, solid-state ^{13}C CP/MAS spectra of TMP-P (Fig. 1b) showed a signal at 130.0 ppm which was attributed to the existence of C-O^+ with pyrylium moiety. The permanent porosity of TMP-P was established by nitrogen sorption isotherm measurement at 77 K in which typical type-I sorption isotherms curves directed its distinctive microporous structures (Fig. 1c). The Brunauer-Emmett-Teller (BET) method was used to evaluate the surface area to be 103.34 m^2/g while its pore size distribution from the adsorption branch mainly centered around 1.245 nm with the NLDFT method (Fig. S1 in Supporting information). For the presence of counter ions, the pore structure was readily blocked, which was generally consistent with the properties of mainly ionic organic porous polymers. The FE-SEM image as shown in Fig. S2 (Supporting information) indicated that TMP-P acquired morphologies of stacked spheres, proving its microporous structures. PXRD pattern of TMP-P was a broad peak, which indicated that the material is amorphous (Fig. S3 in Supporting information). According to TGA, the TMP-P showed excellent thermal stability with 80% of weight at 400 °C and retained more than 50% at 800 °C (Fig. 1d). In addition, the solid-state fluorescence spectrum of TMP-P (Fig. S4 in Supporting information) exhibited its excitation wavelength and emission wavelength at 240 nm and 392 nm respectively, which meant the successful implantation of fluorescent moieties into porous frameworks.

The comparative study of UV–vis diffuse reflection spectra of TMP-P with TMP-M (Fig. 2a) was recorded and showed a broader absorption band in the range of 250-650 nm, which covers the majority of the visible light region and part of the UV region. According to the Kubelka-Munk function equation, the bandgap energy of TMP-P was calculated to be 2.03 eV (Fig. S5 in Supporting information). In addition, the electrochemical Mott-Schottky curve test was carried out to determine the relative position of its valence band (VB) and conduction band (CB). The positive slope in the Mott-Schottky diagrams indicated that TMP-P was an n-type semiconductor (Fig. 2b), and the corresponding CB potential was −0.96V *vs.* SCE. Further, the optical bandgap in combination with the VB of TMP-P was calculated to be 1.07 V *vs.* SCE (Fig. S6 in Supporting information). In general, the pyrylium-based polymer had a strong visible light absorption and its redox potential is sufficient to excite certain molecules to an active state. This result indicated that TMP-P has a great ability to act as a metal-free photocatalyst in visible-light-driven oxidation reactions.

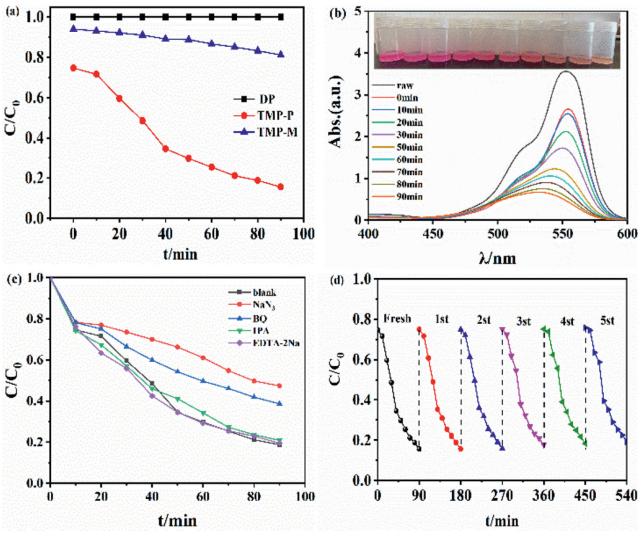

Fig. 3. (a) Photocatalytic degradation of RhB (20 mg/L) over direct light (black), with the catalyst of TMP-P(red) and TMP-M (blue) under visible light. (b) The UV–vis spectra of the RhB (20 mg/L) under various time intervals. inset: images of the mixed dyes solution for pre-fixed time intervals. (c) Effect of different scavengers on the degradation of RhB (20 mg/L), TMP-P control (black), TMP-P with NaN_3 for $^1O_2$ (red), TMP-P with EDTA-2Na for hole (purple), TMP-P with IPA for $^{\bullet}OH$ (green) and TMP-P with BQ for $^{\bullet}O_2^-$ (blue). (d) Recyclability of TMP-P for the photodegradation of RhB (20 mg/L).

As water has a vital role in life on the Earth, the irregular dissemination of water and release of non-treated sewage have durable adversative effects on water resources. Therefore, it is crucial to develop efficient methods to resolve the challenges. The high toxicity, carcinogenicity, and non-biodegradability of organic pollutants in water can create an environmental disaster. It is known that small molecular pyrylium salts can degrade organic pollutants [33], while their poor stability and recyclability are a great hindrance to their futuristic application. Therefore, the heterogeneous pyrylium-based POPs can effectively resolve the problems of stability and recyclability.

Initially, photocatalytic behavior of TMP-P was observed *via* monitoring the concentration of RhB aqueous solution under visible light. The adsorption and desorption equilibrium of TMP-P was achieved in the aqueous solution of RhB before photodegradation tests. The studies revealed that with no catalyst, RhB was hardly degraded under the irradiation of visible light. Besides, under the catalytic activity of TMP-P, the RhB (10 mg/L) showed ~98% degradation within 60 min (Fig. S7 in Supporting information). On the other hand, TMP-M degraded 19% of RhB (20 mg/L) in 90 min (Fig. 3a), meanwhile, TMP-P showed superb degradation of 85% of RhB (20 mg/L) (Fig. 3b), these results indicated that TMP-P has great capability for photodegradation of RhB compared with reported POPs (Table S1 in Supporting information) [34–37]. The photocatalytic degradation rate of TMP-P in RhB (20 mg/L) was confirmed to be by the first-order kinetic equation:

$$-\ln(\rho/\rho_0) = K_{app} \cdot t \quad (1)$$

The relationship between -ln(ρ/ρ_0) and t was linear (Fig. S9 in Supporting information). The reaction kinetic constant of TMP-P degradation was calculated to be 0.0193 min^{-1}.

To get insights into the mechanism of RhB photodegradation by TMP-P, the effects of free radicals and holes in the photocatalytic process were reflected by adding different trapping agents (Fig. 3c). The trapping agents like isopropyl alcohol (IPA), *p*-benzoquinone (BQ), sodium azide (NaN_3), and ethylenediaminetetraacetic acid disodium salt (EDTA-2Na) were respectively added for hydroxyl ($^{\bullet}OH$), superoxide ($^{\bullet}O_2^-$) radicals, singlet oxygen ($^1O_2$) and holes (h^+). In contrast to TMP-P without trapping agents, the removal efficiency of RhB was almost unaffected in the presence of IPA and EDTA-2Na. However, with the addition of BQ and NaN_3, the degradation rate of RhB was decreased by 52.5% and 61% degradation respectively in 90 min, these outcomes indicated that the photocatalytic degradation of RhB by TMP-P was possibly due to the involvement of the generated $^1O_2$ and $^{\bullet}O_2^-$ in the oxidation of the macromolecular dye.

As shown in Fig. 2c, the characteristic absorption peak and the purple-colored 1,4-bis(dimethylamino) benzene-cationic radical solution implied the excellent photocatalytic activity to produce $^{\bullet}O_2^-$ of TMP-P. Then, the $^1O_2$ production capacity of TMP-P was experimentally validated by an electron paramagnetic resonance (EPR) experiment using TEMP as a spin-trapping agent for $^1O_2$. As shown in Fig. 2d, upon exposure to light, TMP-P produced the characteristic 1:1:1 triplet signal due to the formation of the 2,2,6,6-tetramethylpiperidine 1-oxyl (TEMPO) radical by the reaction of TEMP with $^1O_2$.

In the case of photodegradation reusability and recyclability, TMP-P was taken as the photocatalyst to degrade RhB (20 mg/L) in an aqueous solution five times in successive experiments. After five cycles, it was observed that the photocatalytic degradation efficiency of TMP-P remained to be 80% (Fig. 3d). Moreover, FT-IR spectra (Fig. S11 in Supporting information) have certified that there was no change in the structure of TMP-P after several cycles. Therefore, TMP-P displayed robust photodegradation activity and stability, compared with small molecule pyrylium salts with significant practical application.

In summary, TMP was used as the key building block to synthesize a new iPOP through the Knoevenagel condensation reaction. The molecular structure was characterized by FT-IR, ^{13}C NMR, BET, FE-SEM, TGA, and PXRD. The photophysical and electrochemical properties of TMP-P indicated that it has a wider visible light absorption range, smaller bandgap, and retains the fluorescence characteristics of the pyrylium salt monomer. The TMP-P performed excellent photodegradation of 98% RhB (10 mg/L) in 60 min, even with a degradation efficiency of 85% RhB (20 mg/L) within 90 min. The singlet oxygen radical and superoxide radical were confirmed to act as high reactive species at the same time in the photodegradation process. The photocatalytic ability of TMP-P was stable and reusable. It was proved that pyrylium salts can be taken as an effective framework for the development of the new POPs-based metal-free photocatalysts and verified the pyrylium chemistry as a promising synthetic route to fabricate novel POPs with versatile functions Eq. 1.

Declaration of competing interest

The authors declare that they have no known competing financial interests or personal relationships that could have appeared to influence the work reported in this paper.

Acknowledgment

We are grateful for financial support from the Natural Science Foundation of Liaoning Province (No. 2019-MS-046).

Supplementary materials

Supplementary material associated with this article can be found, in the online version, at doi:10.1016/j.cclet.2022.05.055.

References

[1] Y.M. Li, H. Wang, X.P. Li, Chem. Sci. 11 (2020) 12249–12268.
[2] E. Hola, J. Ortyl, Eur. Polym. J. 150 (2021) 110365–110381.

[3] R. Martinez-Haya, M.H. Barecka, P. Miro, M.L. Marin, M.A. Miranda, Appl. Catal. B 179 (2015) 433–438.
[4] R. Martinez-Haya, J. Gomis, A. Arques, et al., J. Hazard. Mater. 356 (2018) 91–97.
[5] R. Martinez-Haya, J. Gomis, A. Arques, et al., Appl. Catal. B 203 (2017) 381–388.
[6] R. Martinez-Haya, M.A. Miranda, M.L. Marin, Catal. Today 313 (2018) 161–166.
[7] K. Wang, L.G. Meng, L. Wang, Org. Lett. 19 (2017) 1958–1961.
[8] C. Sambiagio, M. Ferrari, K. v. Beurden, et al., Org. Lett. 23 (2021) 2042–2047.
[9] N. Corrigan, S. Shanmugam, J.T. Xu, C. Boyer, Chem. Soc. Rev. 45 (2016) 6165–6212.
[10] N.A. Romero, D.A. Nicewicz, Chem. Rev. 116 (2016) 10075–10166.
[11] L. Bao, J.T. Cheng, Z.X. Wang, X.Y. Chen, Org. Chem. Front. 9 (2022) 973–978.
[12] C.L. Cruz, D.A. Nicewicz, ACS Catal. 9 (2019) 3926–3935.
[13] Q. Michaudel, V. Kottisch, B.P. Fors, Angew. Chem. Int. Ed. 56 (2017) 9670–9679.
[14] A.J. Perkowski, W. You, D.A. Nicewicz, J. Am. Chem. Soc. 137 (2015) 7580–7583.
[15] E.H. Discekici, A. Anastasaki, J.R.D. Alaniz, C.J. Hawker, Macromolecules 51 (2018) 7421–7434.
[16] P. Lu, V.K. Kensy, R.L. Tritt, D.T. Seidenkranz, A.J. Boydston, Acc. Chem. Res. 53 (2020) 2325–2335.
[17] S. Wang, H. Li, H. Huang, et al., Chem. Soc. Rev. 51 (2022) 2031–2080.
[18] S.Y. Liu, T.S. Yan, Q.X. Wu, Z. Xu, J. Han, Chin. Chem. Lett. 33 (2022) 239–242.
[19] S. Jiang, L.C. Meng, W.Y. Ma, et al., Chin. Chem. Lett. 32 (2021) 1037–1040.
[20] W.Y. Ji, T.X. Wang, X.S. Ding, S.B. Lei, B.H. Han, Coord. Chem. Rev. 439 (2021) 213875–213903.
[21] T. Takaya, M.D. Mamo, M. Karakawa, Y.Y. Noh, J. Mater. Chem. C 6 (2018) 7822–7829.
[22] D.G. Wang, Q. Li, Y. Zhu, et al., Macromol. Chem. Phys. 218 (2017) 1700101.
[23] W.T. Gong, X.R. Deng, K.X. Dong, L. Liu, G.L. Ning, Poly. Chem. 12 (2021) 3153–3159.
[24] W.T. Gong, K.X. Dong, L. Liu, M. Hassan, G.L. Ning, Catal. Sci. Technol. 11 (2021) 3905–3913.
[25] C. Gu, N. Huang, Y. Chen, et al., Angew. Chem. Int. Ed. 55 (2016) 3049–3053.
[26] O. Buyukcakir, S.H. Je, S.N. Talapaneni, D. Kim, A. Coskun, ACS Appl. Mater. Interfaces 9 (2017) 7209–7216.
[27] M.L. Marin, L. Santos-Juanes, A. Arques, A.M. Amat, M.A. Miranda, Chem. Rev. 112 (2012) 1710–1750.
[28] L. Liu, W.D. Qu, K.X. Dong, et al., Chem. Commun. 57 (2021) 3339–3342.
[29] S. Bi, Z.X. Zhang, F.C. Meng, et al., Angew. Chem. Int. Ed. 61 (2022) e202111627.
[30] X.M. Qian, W.T. Gong, X.P. Li, et al., Eur. J. 22 (2016) 6881–6890.
[31] H. Wang, X. Qian, K. Wang, et al., Nat. Commun. 9 (2018) 1815–1823.
[32] S.Y. Zhang, W.T. Gong, W.D. Qu, et al., Chin. J. Polym. Sci. 38 (2020) 958–964.
[33] S.M. Bonesi, S. Protti, A. Albini, J. Org. Chem. 81 (2016) 11678–11685.
[34] M. Li, H. Zhao, Z.Y. Lu, Microporous Mesoporous Mater 292 (2020) 109774–109783.
[35] P.X. Liu, L.B. Xing, H.T. Lin, et al., Sci. Bull. 62 (2017) 931–937.
[36] L. Huang, Z. Luo, Y.N. Zhou, et al., Mater. Today Chem. 20 (2021) 100475.
[37] N. Xu, R.L. Wang, D.P. Li, et al., Dalton Trans. 47 (2018) 4191–4197.